

# Compositional characteristics of the migmatite gneiss around Awo, southwestern Nigeria

## Značilnosti sestave migmatitnega gnajsa pri Awu v jugozahodni Nigeriji

Mustapha T. Jimoh<sup>1\*</sup>, Anthony T. Bolarinwa<sup>2</sup>, Oluwanifemi O. Ashaye<sup>1</sup>

<sup>1</sup>Department of Earth Sciences, Ladoké Akintola University of Technology, Ogbomoshó, Oyo state, Nigeria

<sup>2</sup>Department of Geology, University of Ibadan, Nigeria

\*Corresponding author. E-mail: mtjimoh@lautech.edu.ng

### Abstract

Migmatite gneiss within the Precambrian basement rocks around Awo, southwestern Nigeria were studied with a view to determine origin and compositional relationship of the paleosomes and neosomes. Other rocks associated with the migmatite gneiss are biotite gneiss, banded gneiss, syenite, granite, pegmatite and aplite. X-Ray Fluorescence geochemical studies reveal minor variations in the bulk chemical composition of paleosomes and neosomes. The composition is dominated by silica ( $w \approx 62\%$ ) and alumina ( $w \approx 15\%$ ). The migmatite gneiss magma type was high K-calc-alkaline to calc-alkaline. The Total Alkali Silica (TAS) plot shows the protolith of the migmatite gneiss to be dioritic and quartz-dioritic rocks while the xenoliths were originally gabbro. The migmatite gneisses are mostly of sedimentary parentage. Trace element data revealed high Ba content, indicating its concentration in felsic minerals. Large Ion Lithophile Elements (LILE) such as Ba, Rb and Sr generally exhibit positive anomaly while High Field Strength Elements (HFSE) notably Ta, Nb, Hf and Zr display weak anomaly. The REE geochemistry revealed strong enrichment of LREE (La, Ce, Pr and Nd) while HREE (Ho, Er, Tm, Yb and Lu) are weakly anomalous. The paleosomes and neosomes of the migmatite gneiss displayed marginal compositional variation which indicates their evolution from the same magmatic source.

**Key words:** Migmatite gneiss, Paleosomes, Neosomes, Geochemistry, Magmatic source

### Izvleček

Migmatitni gnajns v predkambrijskih kamninah podlage v okolici Awa v jugozahodni Nigeriji smo preučevali z namenom opredelitve izvora in primerjave sestave komponent paleosoma in neosoma. Druge kamnine v povezavi z migmatitnim gnajnsom so biotitni gnajns, pasoviti gnajns, sienit, granit, pegmatit in aplit. Rentgenska fluorescenčna preiskava razkriva manjša nihanja celotne kemične sestave paleosoma in neosoma. V sestavi prevladujeta silicijeva ( $w \approx 62\%$ ) in aluminij-ska ( $w \approx 15\%$ ) komponenta. Tip migmatitno gnajns-ove magme je bil visoko K-kalk-alkalni do kalk-alkalni. Diagram celotne alkalne silicije (TAS) nakazuje, da so bile protolit migmatitnega gnajnsa dioritne in kremenovodioritne kamnine, medtem ko so ksenoliti prvotno gabrski. Migmatitni gnajnsi so pretežno sedimentnega porekla. Podatki o sledih razkrivajo visoko vsebnost Ba, očitno koncentriranega v felsičnih mineralih. Velikoionske litofilne prvine (LILE), kot so Ba, Rb in Sr, splošno izkazujejo pozitivno anomalijo, prvine visoke poljske jakosti (HFSE), in sicer Ta, Nb, Hf in Zr, pa šibko anomalijo. Geokemična sestava prvih redkih zemelj priča o znatni obogatitvi LREE (La, Ce, Pr in Nd), medtem ko so HREE (Ho, Er, Tm, Yb in Lu) šibko anomalne. Paleosomi in neosomi migmatitnega gnajnsa kažejo zmerno variacijo sestave, ki priča o njihovem poreklu iz istega magmatskega vira.

**Ključne besede:** migmatitni gnajns, paleosomi, neosomi, geokemija, magmatski izvor

## Introduction

Migmatites are heterogeneous metamorphic rocks consisting of intermingled leucosomes, melanosomes and mesosomes [1, 2]. They are also described as partially melted rocks of the continental crust which is made up of two components the neosomes and paleosomes [3].

Neosomes are crystallized products and residual materials from the melt whereas the paleosomes are the unmelted rocks. The study area which occur within the Precambrian basement complex of south-western Nigeria is located around Awo within Latitude  $7^{\circ} 45' N$  and  $7^{\circ} 4' N$  and Longitude of  $4^{\circ} 23' E$  and  $4^{\circ} 27' E$ . Field investigations showed the occurrence of diverse granitic rocks with structural features consistent with regional trend of the Nigeria basement complex. The various geological units identified around the study area are migmatite gneiss, banded gneiss, biotite gneiss, quartzite, syenite, granite and pegmatite (Figure 1).

The migmatite gneiss is located towards the central portion and the southwestern part of the study area (Figure 1). Field description revealed the migmatite gneiss as a massive outcrop. Xenoliths occur as fine grained mafic inclusions within the gneissic bodies. These inclusions are of various sizes and shapes. The shapes vary from angular, sub-angular, rounded, sub-rounded, lenticular to irregular pods (Figure 3). Odeyemi and Rahaman [4] postulated that the migmatite-gneiss of the basement complex and the meta-supracrustal rocks mark the termination of Precambrian activity in southwestern Nigeria. Migmatite gneiss complex is the oldest, most widespread and abundant rock type in the basement complex [4]. The migmatite gneiss is grayish in color and medium grained in texture, with alternation of mafic and felsic bands set in a medium to coarse grained ground mass. In some locations, pegmatite veins of variable dimensions are intruded into the gneissic bodies. These veins maintain various forms and relationship which are concordant, discordant, cross cutting and contorted with the foliation plane of the gneissic rock. The focus of this study is to investigate the migmatite gneiss with a view to highlighting the compositional characteristics of the paleosomal and neosomal components.

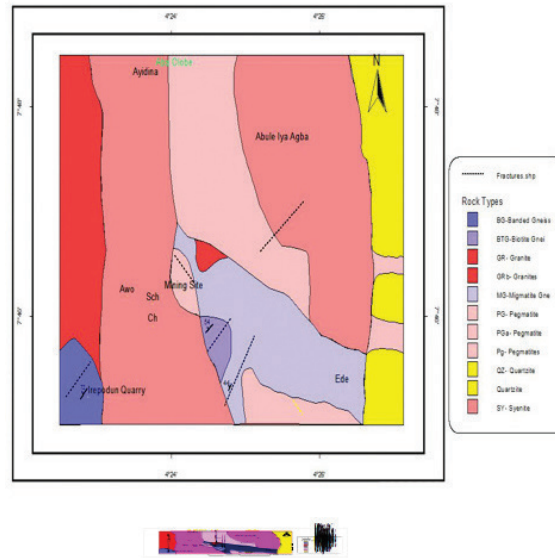


Figure 1: Geological map of the study area.

### Geological Settings and Field Characteristics

Various geological units associated with the migmatite gneiss are banded gneiss, biotite gneiss, granite, syenite and pegmatite. Of all the rock types occurring in the study area, migmatite gneiss and biotite gneiss appear to be predominant while banded gneiss, syenite, granite and pegmatites occur in subordinate proportion. Migmatite gneisses are the oldest and most widespread lithology within the study area. They form the country rock in which all other rocks intrude. They are well exposed with mostly flat lying outcrop. They also cut across river and stream channels as highly weathered rocks. The migmatite gneisses are not treated as a single lithological unit they were segregated into paleosomes and neosomes. Neosomes are further segregated into leucosomes and melanosomes. (Table 1). The leucosomes are quartzofeldspathic in composition. Quartz appears dominant in the mode ( $> 70\%$ ). The melanosomes contain varying amount of ferromagnesian minerals like platy biotite, prismatic hornblendes and equant pyroxene. Melanosomes are also identified as xenoliths. The presence of pyroxene confers a greenish tint on the rock body. The composite fabrics of paleosomes and neosomes are folded on mesoscopic scale. The paleosomes and leucosomes are concurrently folded and terminate abruptly into what appears as an enclave

or tight isoclinal fold (Figure 2). The trends of the fold axis are mostly east- west. Lineation plunges usually to the north, reflecting ductile deformation. Deformations are mainly ductile. Fragments of enclaves or raft structure (competent materials) are enveloped within less competent components. The enclaves are mainly mafic subordinately felsic. These enclaves are of various shapes and sizes. Large number of shear planes was recognized in the study area, shearing was identified due to fabrics of the tectonically deformed rocks. Shearing had led to formation of various structural features like reorientation due to rotation, boudins and lenses (Figure 2). Enclaves are rock fragments that resisted migmatization (resisters) or residual materials from which mobile materials have been extracted [5, 6].

## Materials and Methods

Geological mapping of Awo area was conducted on a scale of 1 : 50 000. Particular attention was taken for the location, physical characteristics,

mineral constituents, structural elements and associated rocks of the migmatite gneiss. Sampling was done to preserve various structures within the migmatite gneiss for future studies. A few samples were collected from each rock body for geochemical analysis. Various field measurements were used during the mapping. Global Positioning System (GPS) was used for geographical positioning with respect to various outcrops available in the study area. Measurement of strike, dip, plunge of structures such as foliation, lineation and fold axis were made. Field descriptions and observation were adequately recorded in a field notebook. Samples collected were properly labeled and stored prior to analyses. Representative rock samples were pulverized at Geochemistry Laboratory, Department of Geology of the University of Ibadan and analyzed at ACME Laboratory, Ontario, Canada using X-Ray Fluorescence (XRF) methods. Geochemical data were processed using Petrographic software package for different geochemical variation and discrimination diagrams.

**Table 1:** Chemical composition of the Migmatite gneiss of Awo

Analyte	NEOSOME								PALEOSOME					
	Major element concentration in mass fractions, w/%													
	RS1	RS2	RS3	RS4	RS5	Mean	Range	RS6	RS7	RS8	RS9	Mean	Range	
SiO <sub>2</sub>	44.5	55.5	58.7	61.5	61.5	56.34	61.5–44.5	65.1	63.8	65.3	74.2	67.1	74.2–63.8	
Al <sub>2</sub> O <sub>3</sub>	12.54	14.77	14.93	14.49	15.16	14.38	15.16–12.54	14.96	14.39	14.43	15.50	14.82	15.50–14.39	
Fe <sub>2</sub> O <sub>3</sub>	18.10	8.47	11.29	5.72	9.34	10.60	18.10–5.72	6.22	7.80	7.34	0.39	5.44	7.80–0.39	
CaO	6.31	7.36	2.26	4.67	2.50	4.62	7.36–2.50	3.09	2.92	2.00	0.43	2.11	3.09–0.43	
MgO	7.65	6.63	3.94	5.40	3.35	5.40	7.65–3.35	2.23	2.86	2.55	0.08	1.93	2.86–0.08	
Na <sub>2</sub> O	0.52	2.69	2.35	2.95	2.82	2.27	2.95–0.52	3.46	2.94	3.42	7.14	4.24	7.14–2.94	
K <sub>2</sub> O	5.32	2.20	4.15	3.15	3.66	3.70	5.32–2.20	2.57	3.03	3.15	1.90	2.66	3.15–1.90	
MnO	0.39	0.17	0.21	0.16	0.15	0.22	0.39–0.15	0.12	0.15	0.15	0.11	0.13	0.15–0.11	
TiO <sub>2</sub>	2.43	2.08	1.77	0.74	1.32	1.47	2.43–0.74	1.00	1.30	1.22	0.04	0.89	1.30–0.04	
P <sub>2</sub> O <sub>5</sub>	0.58	0.49	0.06	0.62	0.04	0.36	0.62–0.04	0.11	0.13	0.07	0.20	0.13	0.20–0.07	
LOI	1.67	0.37	0.73	0.54	0.64	0.79	1.67–0.37	0.47	0.56	0.49	0.52	0.51	0.56–0.47	
<b>Total %</b>	<b>100.01</b>	<b>99.73</b>	<b>100.39</b>	<b>99.94</b>	<b>100.48</b>			<b>99.33</b>	<b>99.88</b>	<b>100.12</b>	<b>100.51</b>			

Analyte	NEOSOME							PALEOSOME						
	Trace element concentration ( $\times 10^{-6}$ )													
	RS1	RS2	RS3	RS4	RS5	Mean	Range	RS6	RS7	RS8	RS9	Mean	Range	
Cu	20	10	70	10	10	24	70–10	20	10	10	10	13	20–10	
Ni	270	110	100	40	90	122	270–40	10	40	30	10	11	40–10	
Pb	10	10	10	10	10	10	10	10	10	10	10	10	10	
Zn	250	110	160	120	110	150	250–110	10	110	110	40	68	110–10	
Zr	161	186	425	189	231	238	231–161	251	307	367	24	242	367–24	
Ba	706	478	992	871	638	737	992–478	647	891	667	42	562	891–42	
Be	2	36	7	2	51	20	51–2	4	2	4	6	4	6–2	
Co	38	32	32	27	23	30	38–23	18	18	20	1	14	20–1	
Cs	4	20	4	3	30	12	30–3	2	2	3	4	3	4–2	
Ga	26	19	21	21	20	54	54–19	18	20	19	22	20	22–18	
Rb	187	166	159	137	245	179	245–137	94	116	141	158	127	158–94	
Sn	6	4	1	2	3	3	6–1	1	1	6	11	5	11–1	
Sr	68	277	297	393	356	267	356–68	303	299	247	10	215	303–10	
V	261	182	203	188	78	182	261–78	100	135	125	10	93	135–101	
Hf	5	5	12	5	6	7	12–5	8	11	10	1	8	11–1	
Nb	40	30	30	26	37	31	40–26	15	16	26	20	19	20–15	
Ta	2	6	1	1	11	4	11–1	1	1	1	1	1	1	
Th	2	14	32	31	20	20	32–2	25	29	16	2	18	29–2	
U	2	6	2	1	10	4	10–1	1	1	2	5	2	5–1	
W	1	3	2	2	5	3	5–1	2	1	1	4	2	4–1	
Y	62	30	24	20	24	32	62–20	23	25	13	6	17	25–6	

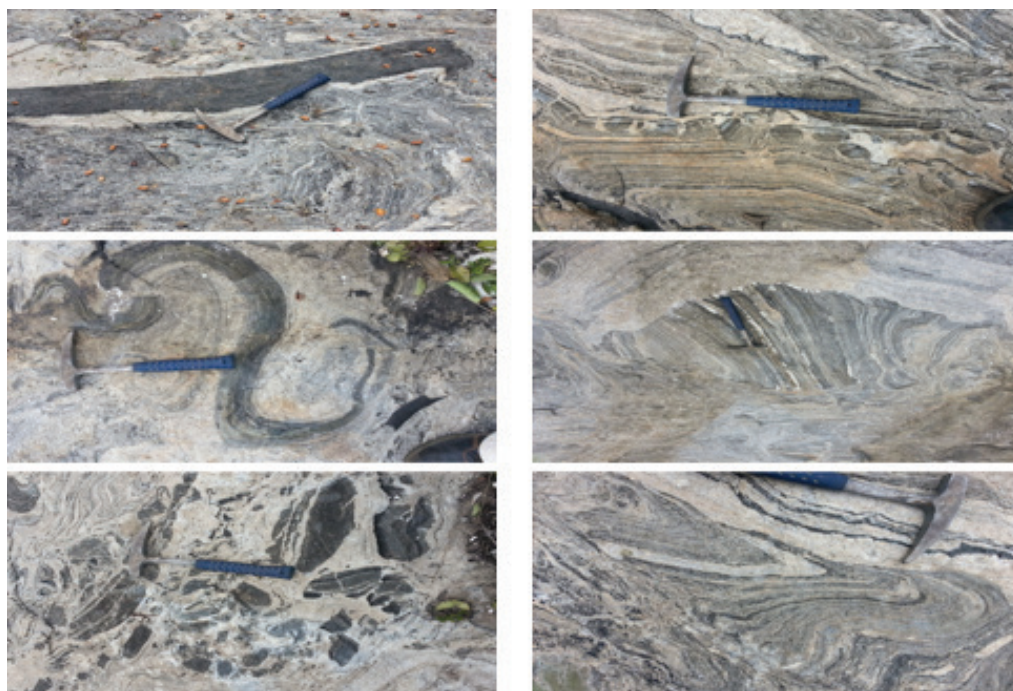


**Figure 2:** Migmatite gneiss showing various structures: top left - basic dyke; top right - sheared boudins; middle left - rotated and folded metabasic rocks; middle right - symmetrical tail of leucosome around an enclave of melanosome; bottom left - randomly oriented raft structure of basic dykes embedded in matrix of leucosome; bottom right - tight folding of foliated paleosome, leucosome and melanosome.



## Results and Discussion

### Major Element Geochemistry

Nine representative samples of the paleosomes and neosomes were selected to determine their major, trace and rare earth elements geochemistry. Five of the samples were taken from paleosomes and four from neosomes (Table 1). The xenolith expectedly has very low concentration of  $\text{Na}_2\text{O}$  ( $w = 0.52\%$ ), and much higher concentrations of  $\text{K}_2\text{O}$  ( $w = 5.32\%$ ) and a proportionately high concentration of  $\text{Fe}_2\text{O}_3$  ( $w = 18.10\%$ ) and  $\text{MgO}$  ( $w = 7.65\%$ ) due to its mafic composition (Table 1). The paleosomes and neosomes of the migmatite gneisses are compositionally different in their mean values as revealed by major oxide data presented in Table 1. The lowest mean value of  $\text{SiO}_2$  is  $w = 44.5\%$  which indicates the mafic nature of the paleosomes while the highest mean value of  $\text{SiO}_2$  is  $w = 74.2\%$  which as well reveal the felsic nature of the neosomes. Low range values of oxides such as  $\text{Na}_2\text{O}$  ( $w = 2.95\text{--}0.52\%$ ) and high range values of  $\text{Fe}_2\text{O}_3$  and  $\text{MgO}$  ( $w = 18.10\text{--}5.72\%$  and  $w = 7.65\text{--}3.35\%$ ) further affirm the mafic composition of the paleosomes. The overall trend for all major elements suggests that the paleosomes evolved from parent material which is intermediate between felsic and mafic sources. This is evident from the moderately high concentration of  $\text{SiO}_2$  in the range of  $w = 61.5\text{--}44.5\%$  while a range value of  $w = 74.2\text{--}63.8\%$  for neosomes clearly indicates its felsic precursor. High contents of  $\text{Fe}_2\text{O}_3$  ( $w = 18.10\text{--}5.72\%$ ) for paleosomes attest the basic nature of the parent materials, while low Fe content ( $w = 7.80\text{--}0.39\%$ ) in neosome indicates its felsic parentage. The mean values of  $\text{Na}_2\text{O}$  and  $\text{K}_2\text{O}$  (Table 1) for the paleosomes and neosomes reflect the abundance of K-rich rock forming silicates like biotite and microcline [7]. The paleosome and neosome show slight variation in their sources. The paleosomes are derived from diorite and syenodiorite sources whereas the neosomes are mostly derived from quartz diorite and granite sources (Figure 3). The AFM diagrams [9, 10] were used to determine whether the rock samples are derived from tholeiitic or calc-alkaline rock suite, the major element data were plotted on triangular diagram comprising of A ( $\text{Na}_2\text{O} + \text{K}_2\text{O}$ ), F ( $\text{FeO} + \text{Fe}_2\text{O}_3$ ) and M ( $\text{MgO}$ ).

The plot falls within calc-alkaline rock suite which is rich in  $\text{Na}_2\text{O}$ ,  $\text{K}_2\text{O}$  and total Fe but low in  $\text{MgO}$  (Figure 3). The AFM diagrams were also employed to investigate the enrichments of the paleosomes and neosomes in  $\text{Na}_2\text{O}$ ,  $\text{K}_2\text{O}$ ,  $\text{MgO}$  and total Fe. The paleosomes are moderately enriched in  $\text{MgO}$  and total Fe while the neosomes are highly enriched in  $\text{Na}_2\text{O}$  and  $\text{K}_2\text{O}$  with low amount of total Fe (Figure 3). It is further confirmed by the plot of  $\text{SiO}_2$  versus  $\text{Na}_2\text{O} + \text{K}_2\text{O}$  [8] which revealed that the migmatite gneiss originates from dioritic rocks (Figure 3).  $\text{SiO}_2$  was plotted against  $\text{K}_2\text{O}$  adopting the model of Pecerillo and Taylor [13] to further determine if the rock series is high or medium calc-alkaline (Figure 3). In term of tectonic setting, following the model of Pearce et al [17] where Rb was plotted against Y + Nb, the neosome plots in the field of Volcanic Arc Granite while the paleosome plots in Within Plate Granite (Figure 3). Both components are thus product of post-collisional tectonic setting. Most of the values plot within field of high-K calc-alkaline series. Furthermore, all the major oxides were plotted against  $\text{SiO}_2$  in Harker's diagram (Figure 4) because  $\text{SiO}_2$  is regarded as fractionation index for the evolution of magma and the most abundant oxide in igneous rocks that exhibit a wide variation in composition [11].  $\text{Al}_2\text{O}_3$  and  $\text{Na}_2\text{O}$  are positively correlated with  $\text{SiO}_2$  which is an indication of possible separation of felsic minerals like sodic plagioclase during fractional crystallization [12].  $\text{Fe}_2\text{O}_3$ ,  $\text{CaO}$ ,  $\text{K}_2\text{O}$  and  $\text{MgO}$  versus  $\text{SiO}_2$  were negatively correlated and indicate a separation of ferromagnesian minerals during crystallization (Figure 4).

Various models were used to determine the ancestry of the migmatite gneiss. Awo migmatite gneiss on the  $\text{Na}_2\text{O}/\text{Al}_2\text{O}_3$  vs  $\text{K}_2\text{O}/\text{Al}_2\text{O}_3$  plot was used to discriminate between igneous and sedimentary/metasedimentary rocks [14]. Approximately 90% of the plots fell within sedimentary/metasedimentary field (Figure 5). Similarly, the  $\text{K}_2\text{O}$  vs  $\text{Na}_2\text{O}$  plot [8] showed an overwhelming 90% of the values plotting within eugeosynclinal sandstones field (Figure 5). Furthermore, in the  $\text{TiO}_2$  vs  $\text{SiO}_2$  diagram [16], the plot fell within sedimentary field which suggests that the protolith of the migmatite gneiss has been grossly affected by crustal contamination (Figure 5).

**Trace and Rare Earth Elements Geochemistry**

Trace element concentrations of the paleosome and neosome are presented in Table 1. The concentrations of Large Ion Lithophile Elements (LILE) such as Ba, Rb and Sr for paleosomes and neosomes are enriched, but the mean values are slightly higher in paleosome than neosome (Table 1). The concentrations of High Field Strength Elements (HFSE) like Ta, Nb and Hf are generally depleted; neosomes are more depleted in HFSE than paleosomes. However Zr is moderately enriched compared to other HFSE (Table 1). For trace elements, high content of Ba with mean values of  $737 \times 10^{-6}$  and

$562 \times 10^{-6}$  for paleosome and neosome respectively (Table 1) are conspicuously discernible which indicates its concentration in felsic minerals. This attests to granitic origin of the rock samples. The assertion is further corroborated by moderate amount of Rb ( $179 \times 10^{-6}$  and  $127 \times 10^{-6}$ ) and Zr ( $238 \times 10^{-6}$  and  $242 \times 10^{-6}$ ) for paleosomes and neosomes respectively which are concentrated in rocks of acidic or intermediate composition. The LILE such as Ba, Rb and Sr generally exhibit positive anomaly, while HFSE such as Ta, Nb, Hf and Zr display weak anomaly (Figure 6).

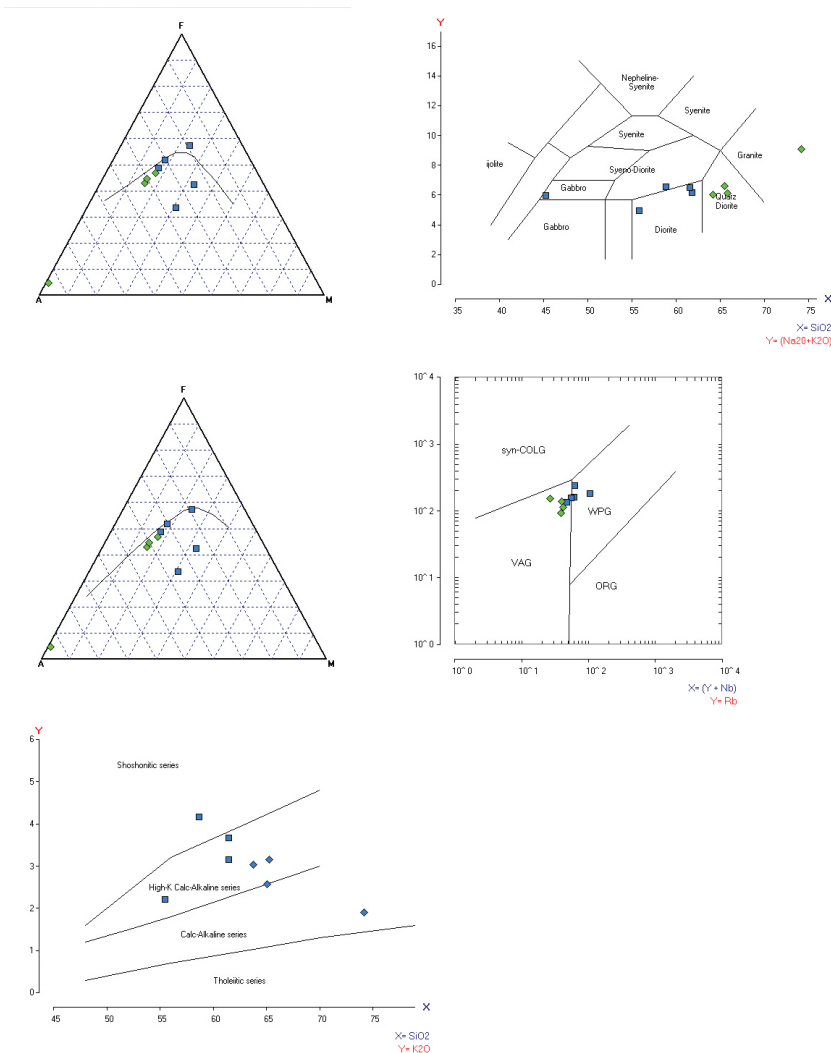


**Figure 3:** Top left - AFM diagrams (after Irvine and Baragar<sup>[10]</sup>); middle left – (after Kuno<sup>[9]</sup>); top right - Plot of  $Na_2O K_2O$  versus  $SiO_2$  (after Cox et al<sup>[8]</sup>); middle right -  $K_2O$  versus  $SiO_2$  plot (after Peccerillo and Taylor<sup>[13]</sup>); bottom - Rb versus Y + Nb tectonic discrimination diagram (after Pearce et al<sup>[17]</sup>).

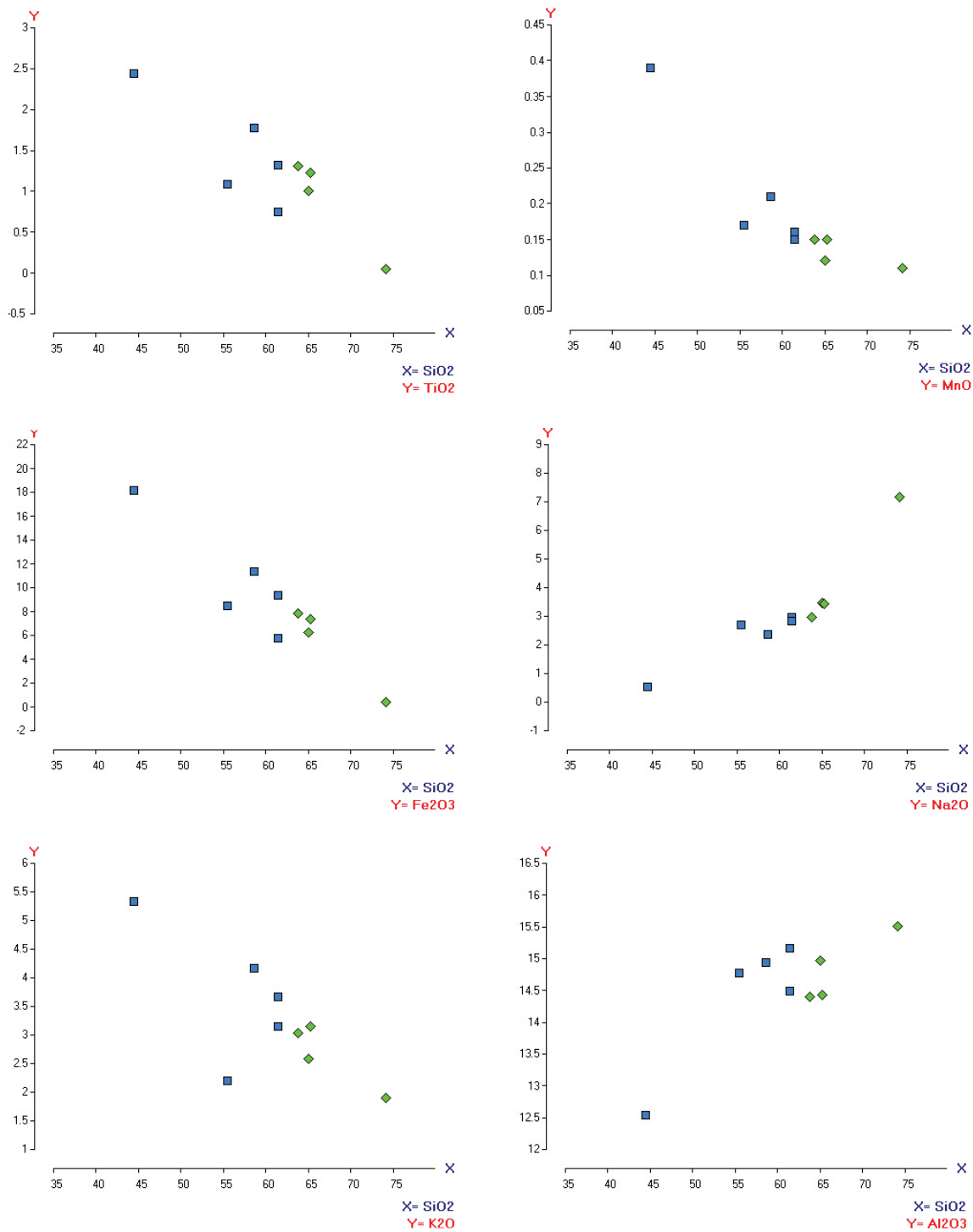


Figure 4: Harker's variation plot of SiO<sub>2</sub> versus other major elements

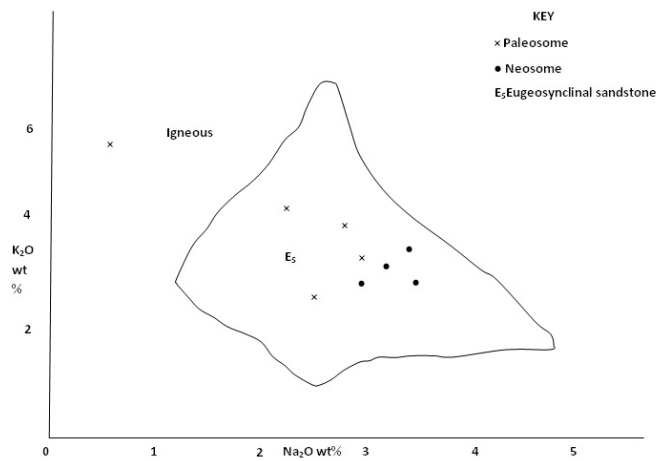
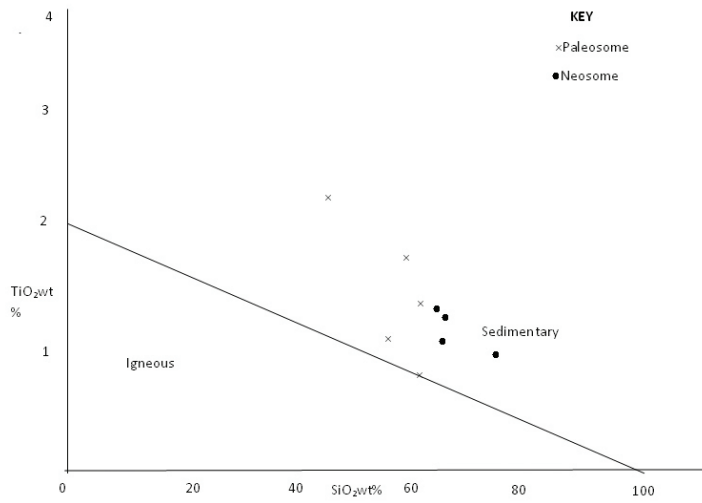


Fig..... K<sub>2</sub>O vs Na<sub>2</sub>O plot of the migmatite gneiss around Awo (after Middleton, 1960).

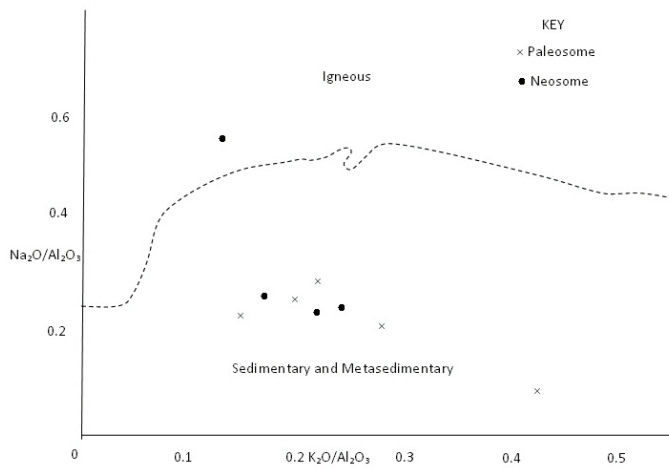
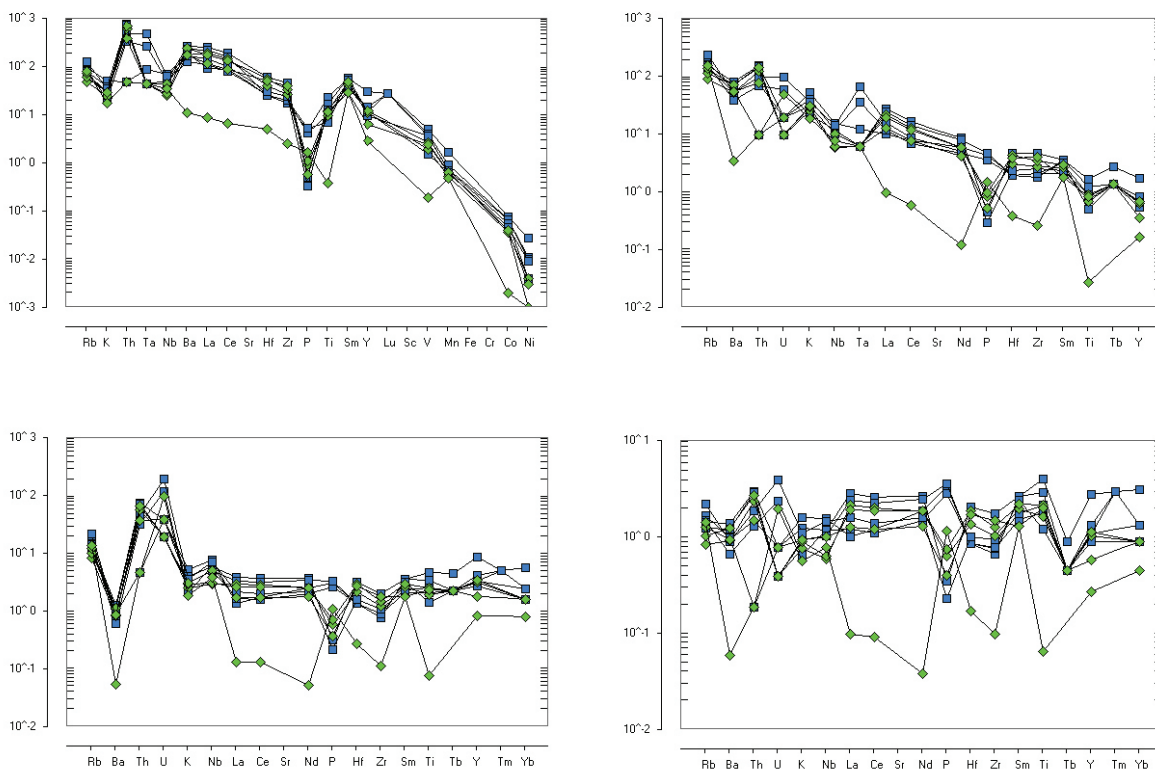


Figure 5: Top - TiO<sub>2</sub> versus SiO<sub>2</sub> plot (after Tarney<sup>[16]</sup>); middle - K<sub>2</sub>O vs Na<sub>2</sub>O plot (after Middlemost<sup>[15]</sup>); bottom - Na<sub>2</sub>O/Al<sub>2</sub>O<sub>3</sub> versus K<sub>2</sub>O/Al<sub>2</sub>O<sub>3</sub> diagram (after Garrels and Mackenzie<sup>[14]</sup>).





**Figure 6:** Left - Mantle normalized pattern of trace elements for Paleosome and neosome (after Wood et al<sup>[18]</sup>); right - Chondrite normalized pattern of rare earth elements for paleosomes and neosomes after Haskin et al<sup>[19]</sup>.

The enrichment in LILE and depletion in HFSE reflect geotectonic setting from which the rocks originated. The setting suggests the rocks to evolve in a process of subduction. REE concentrations of the paleosomes and neosomes as presented in Table 1 reveal strong positive anomaly for LREE such as La, Ce, Pr and Nd while HREE like Ho, Er, Tm, Yb, and Lu show weak anomaly. Source materials of the migmatite gneiss can be inferred from trace and rare earth element patterns<sup>[12]</sup>. The moderately enriched LREE and weakly negative Eu anomaly possibly suggest the melt to have been derived from rocks of intermediate composition like diorite and quartz diorite (Figures 5 and 6).

## Conclusion

The study area occurs within metamorphic terrane of the south western basement complex of Nigeria. Formation of different rock types around the area is probably connected to post-collisional events that influenced the structural and textural features of the various

geological units. The available geochemical data from the study area suggest the paleosomes and neosomes to be mostly of sedimentary parentage with minor input from igneous protolith (Figure 5). The paleosome and neosome bear compositional similarities. However, minor petrological differences exist between each component. The differences are associated with the composition of their sources and crustal contamination during the transportation of the melted materials. The migmatite gneiss is derived from rocks of dioritic composition belonging to calc-alkaline series. Negative correlation between  $\text{SiO}_2$  and major elements like  $\text{Fe}_2\text{O}_3$ ,  $\text{CaO}$ ,  $\text{K}_2\text{O}$  and  $\text{MgO}$  indicate a pronounced effect of fractional crystallization during the formation of the dioritic rocks. Large Ion Lithophile Elements (LILE) such as Ba, Rb and Sr generally exhibit positive anomaly while High Field Strength Elements (HFSE) notably Ta, Nb, Hf and Zr display negative anomaly. The REE geochemistry revealed strong positive anomaly for LREE (La, Ce, Pr and Nd) while HREE (Ho, Er, Tm, Yb and Lu) are weakly anomalous. Evidence from geochemical data coupled with pat-

terns of major, trace elements and rare earth elements revealed that the paleosomes and neosomes have common magmatic and geotectonic source.

## References

- [1] Allen, T. T. (1992): *Migmatite Systematics and Geology Carter Dome - Wild River Region, White Mountains, New Hampshire*. Ph. D. Thesis, Dartmouth College.
- [2] Sawyer, E. W. (2008) *Identifying parts of Migmatites in the Field*. In Sawyer E.W and Brown M (eds) Working with Migmatites. Mineralogical Association of Canada, Short Course; 38, pp. 29–36.
- [3] Sawyer, E. W., Cesare, B., Brown, M. (2011): When the Continental Crust Melts. *Mineralogical Society of America*; 7 (4), pp. 229–234.
- [4] Odeyemi, I. B., Rahaman, M. A. (1992): The Petrology of a Composite Syenite dyke in Igarra, Southwestern Nigeria. *Journal of Mining and Geology*; 28 (2), pp. 255–264.
- [5] Shelley, D. (1997): *Igneous and Metamorphic rocks under microscope*. Chapman & Hall, pp.1–445.
- [6] Pereira, M. F., Silva, J. B. (2002): The Geometry and Kinematics of Enclaves in sheared Migmatites from the Evora Massif, Ossa-Morena zone (Portugal). *Geogaceta*; 31 pp. 193–196.
- [7] Oyinloye A. O. (2011): Geology and Geotectonic Setting of the Basement Complex Rocks in Southwestern Nigeria: *Implications on Provenance and Evolution, Earth and Environmental Sciences*, Dr Imran Ahmad Dar (Ed), pp. 97–118.
- [8] Cox, K. G., Bell, J. D., Pankhurst, R. J. (1979): *The Interpretation of Igneous rocks*. London, George Allen and Unwin, 450 p.
- [9] Kuno, H. (1968): Differentiation of basalt magmas. In: Hess H. H. and Poldervaart A. (eds), *Basalts: The Poldervaart treatise on rocks of basaltic composition*; 2, Interscience, New York, pp. 623–688.
- [10] Irvine, T. N., Baragar, W. R. A. (1971): A guide to the chemical classification of the common volcanic rocks. *Journal of Petrology*; 17, pp. 589–637.
- [11] Wilson, M. (1989): *Igneous Petrogenesis. A Global Tectonic Approach*, Unwin Hyman, London, 466 p.
- [12] Maulana, A., Watanabe, K, Imai, A., Yonezu, K. (2012): Petrology and Geochemistry of Granitic Rocks in South Sulawesi, Indonesia: *Implication for Origin of Magma and Geodynamic Setting*. *World Academy of Science, Engineering and Technology*; 61, pp. 8–13.
- [13] Peccerillo, A., Taylor, S. R. (1976): Geochemistry of Eocene calc-alkaline volcanic rocks from the Kastamonu area, northern Turkey. *Contrib. Mineral. Petrol.*; pp. 63–81.
- [14] Garrels, R. M., Mackenzie, F. T. (1971): *Evolution of sedimentary rocks*. W. W. Norton & Co. Inc. New York, 394 p.
- [15] Middlemost, E. V. (1960): Chemical composition of sandstone. *Bulletin Geological Society of America*; 71, pp. 1011–1026.
- [16] Tarney, J. (1977): Petrology, mineralogy and geochemistry of the Falkland Plateau basement rocks, site 330, deep sea drilling project, *Initial Report*; 36, pp. 893–921.
- [17] Pearce, J. A., Harris, N. B. W., Tindle, A. G. (1984): Trace element discrimination diagrams for the tectonic classification of granitic rocks. *Journal of Petrology*; 25, pp. 956–983.
- [18] Wood, D. A., Joron, J. L., Treuil, M., Norry, M., Tarney, J. (1979): Elemental and Sr isotope variations in basic lavas from Iceland and the surrounding ocean floor. *Contrib. Mineral. Petrol.*; 70, pp. 319–329.
- [19] Haskin, L. A., Haskin, M. A., Frey, F. A., Wildman, T. R. (1968): Relative and Absolute terrestrial abundances of rare earths. In: *Ahrens L.H. (ed) Origin and Distribution of the elements*; 1, Pergamon, Oxford, pp. 889–911.